EFFECT OF OPERATING PARAMETERS OF HYDRAULIC FRACTURING ON FRACTURE GEOMETRY AND FLUID EFFICIENCY IN OLIGOCENE, OFFSHORE VIETNAM

Nguyen Huu Truong

Petro Vietnam University, Vietnam
E-mail: truongbiennho@gmail.com

ABSTRACT: *In the past decades, a large amount of oil production in the Cuu Long basin was mainly exploited from the basement reservoir, oil production from the Miocene sandstone reservoir and a small amount of oil production from the Oligocene sandstone reservoir. Many discovery wells and production wells in lower Tra Tan and Tra Cu of Oligocene sandstone had high potential for oil and gas production and reserve where the average reservoir porosity was in range of 10% to 18%, and reservoir permeability was in range of 0.1 md to 5 md. Due to high reservoir heterogeneity, complication and complexity of the geology, high closure pressure was up to 7,700 psi. The problem in the Oligocene reservoir is very low fracture conductivity due to low conductivities among the fractures of the reservoirs. The big challenges deal with this problem of hydraulic fracturing stimulation to improve oil and gas production that is required of the study. In this article, the authors have presented the effects of operating parameters as injection time, injection rate, and leak-off coefficient of hydraulic fracturing based on the 2D PKN-C fracture geometry account for leak-off coefficient, spurt loss in terms of power law parameters on the fracture geometry. By the use of design of experiments (DOE) and application of response surface methodology in the constraint of operating hydraulic fracturing parameter of the field experience, the effects plots are evaluated. In the recent years, from the successful application of the hydraulic fracturing stimulation for well completion in the Oligocene reservoir, this technology is often used to stimulate reservoir.*

Key words: Operating parameters of hydraulic fracturing, the 2D PKN-C fracture geometry, fluid efficiency.

OLIGOCENE RESERVOIR DESCRIPTION

Energy demand for oil and gas are increasing worldwide and energy supplies for the developing domestic economy is also rising in particular. In the past decades, hydraulic fracturing stimulation has been widely used in the petroleum industry for improving oil production which is to apply stimulation in the vertical well, multistage hydraulic fracturing in a horizontal well. In Vietnam, oil production rate in the Oligocene reservoir declined in a long time due to many reasons such as pressure of the reservoir decline as well as the decrease in oil production rate, the low reservoir permeability from 0.1 md to 5 md, low reservoir porosity from 10% to 18%, reservoir heterogeneity, complicated and complex reservoir. These problems in the reservoir lead to low conductivity among the fractures of the reservoir. They are solved by stimulating the reservoir of hydraulic fracturing stimulation. In

Cuu Long basin, there are three pay zones of oil production that consist of the basement reservoir, Miocene sandstone reservoir, and the Oligocene sandstone reservoir. The previous report has estimated the amount of oil production reserves that can be exploited from the basin about 5600 million to 5950 million barrels of oil equivalent. That is equal to potential hydrocarbon reserves about 22.4 billion to 23.8 billion of oil equivalents. At the basin, 70% of oil production is exploited in the fracture basement reservoir, 18% oil production in the Oligocene reservoir (1033 million barrels of oil reserves) and 12% of oil production in the Miocene reservoir. On the other hand, total amount of oil production in Oligocene reservoir in the White Tiger oil field is only exploited of 76.7 million barrels of oil which is equal to 4.6% of total amount of oil production in the White Tiger and equal to 7.4 % of oil in the Oligocene reservoir. These layers in the Oligocene reservoir include Tra Tan of Oligocene C, Oligocene D and Oligocene E, Tra Cu in the Oligocene F. In this article, the authors have mentioned the Oligocene E reservoir and have presented the effects of operating parameters of hydraulic fracturing on the fracture geometry as fracture half-length, fracture width during fracturing operation in the Oligocene reservoir. The result of the research is very useful in order to select the good operating parameters of hydraulic fracturing in the Oligocene stimulation. In the future work, the authors will present the combined operating parameters of hydraulic fracturing and other parameters that cannot be controlled such as reservoir permeability, fracture height, reservoir porosity affecting to the economic performance.

FRACTURING FLUID SELECTION AND FLUID MODEL

Ideally, the fracturing fluid is compatible with the formation of rock properties, fluid flow in the reservoir, reservoir pressure, and reservoir temperature. Fracturing fluid generates pressure in order to transport proppant slurry and open fracture, produce fracture growth and fracture propagation during

pumping, also fracturing fluid should minimize pressure drop alongside and inside the pipe system in order to increase pump horsepower with the aim of increasing a net fracture pressure to produce more and more fracture dimension. In fracturing fluid system, the breaker additive would be added to the fluid system to clean up the fractures after treatment. Due to high temperature of Oligocene E reservoir the Dowell YF 660 high temperature (HT) without breaker with 2% KCl is selected for fracturing fluid system. To predict precisely the fracture geometry as fracture half-length, fracture width during pumping, the power law fluid model would be applied in this study. Then the most fracturing fluid model is usually given by:

$$\tau = K\gamma^n \tag{1}$$

Where: τ - shear stress, γ - shear rate, K - consistency coefficient, n - rheological index as flow behavior index of non-dimensional model but related to the viscosity of the non-Newtonian fracturing fluid model (Refer to Valko's & Economides, 1995) [1].

The power law model can be expressed by:

$$\text{Log } \tau = \log K + n \log \gamma$$

$$Slope = \left[\left(N \sum XY \right) - \left(\sum X \sum Y \right) \right] \Big/ \left[\left(\sum X^2 \right) - \left(\sum X \right)^2 \right]$$

$$Intercept = \left(\sum Y - n \sum X \right) \Big/ N$$

Where: $X = \log \gamma$, $Y = \log \tau$, and N = Data number. Thus n = Slope and K=Exp (Intercept).

$$\text{Log } \tau = \log K + n \log \gamma$$

$$Slope = \left[\left(N \sum XY \right) - \left(\sum X \sum Y \right) \right] \Big/ \left[\left(\sum X^2 \right) - \left(\sum X \right)^2 \right]$$

$$Intercept = \left(\sum Y - n \sum X \right) \Big/ N$$

Where $X = \log \gamma$, $Y = \log \tau$, and N = Data number. Thus n = Slope and K=Exp(Intercept).

Table 1. Oligocene reservoir data of X well, offshore Vietnam [2]

Parameter	Value
Target fracturing depth, ft.	12,286
Reservoir drainage area, acres	122
Reservoir drainage radius, ft.	1,300
Wellbore radius, ft.	0.328
Reservoir height, ft.	72
Reservoir porosity	0.121
Reservoir permeability, md	0.5
Reservoir fluid viscosity, cp	1.5
Oil formation volume factor, RB/STB	1.4
Total compressibility, psi^{-1}	1.00×10^{-5}
Young's modulus, psi	5×10^6
Sandstone Poisson's ratio	0.25
Initial reservoir pressure, psi	4,990
Reservoir temperature, ^{0}F	266
Oil API	36.7
Gas specific gravity	0.79
Bubble point pressure, psi	1,310
Flowing bottom hole pressure, psi	3,500
Closure pressure, psi	7,700

Table 2. Hydraulic fracturing parameters [2]

Parameter	Value
Fracture height, h_f, ft.	72
Sandstone Poisson's ratio	0.25
Leak-off coefficient, ft/min$^{0.5}$	0.003
Young's modulus, psi	3.00×10^6
Injection rate, bpm	18 bpm to 22 bpm
Injection time, min	60 minutes to 120 minutes
Spurt loss, gal/ft^2	0
Proppant concentration end of job, ppg	8
Flow behavior index, n	0.69
Consistency index, K, lbf.s^n/ft^2	0.04
Fracturing fluid type: Dowell YF 660 HT without breaker with 2% KCI	

PROPPANT SELECTION

In order to select proppant, the proppant would be selected correctly as proppant type, proppant size, proppant porosity, proppant permeability and proppant conductivity, strength proppant under effective stress pressure of the fracture in order to evaluate precisely the fracture conductivity of the fractures with proppant damage factor effect. Proppant is used to open fractures and maintain the open fractures for a long time in high fracture conductivity while pump pressure is shut down and fracture begins to close due to effective stress and overburden pressure. The idea for proppant selection would be stronger to resist the crush, erosion, and corrosion in the well. Due to closure pressure up to 7,700 psi, proppant should be selected as Carbolite ceramic proppant with proppant size 20/40 (Refer to Nolte and Economides) [3].

Table 3. CARBO-LITE ceramic intermediate strength proppant, 20/40

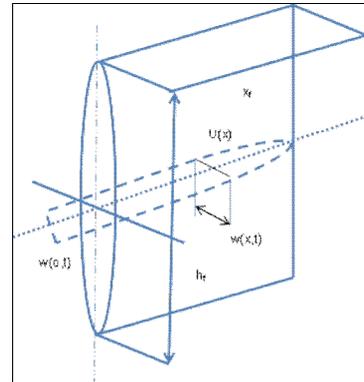| Parameters	Values
Proppant type	20/40 CARBO-Lite
Density, ρ_p	2.71
Strength	Intermediate
Average proppant diameter	0.0287
Proppant porosity, ϕ_p, %	35
Proppant pack permeability, mD	600
Proppant conductivity at closure pressure of 2lb/ft^2	6600 mD.ft
Fracture conductivity damage factor	0.5

FRACTURE GEOMETRY MODEL

Fig. 1. The PKN fracture geometry

In this study, the 2D PKN fracture geometry model (Two dimensional PKN; Perkins and Kern, 1961; Nordgren, 1972) [4, 5] in figure 1 is used to present the significant fracture geometry of hydraulic fracturing stimulation for low permeability, low porosity and poor conductivity as Oligocene E reservoir, that requires the fracture half-length of the fracture design and precise evaluation of the fracture geometry. After incorporation of carter

Solution II, the model known as 2D PKN-C (Howard and Fast, 1957) [6] had incorporated the leak-off coefficient, in terms of consistency index (K), flow behavior index (n), injection rate, injection time, fluid viscosity, fracture height. The model detail referred to (Valko's and Economides, 1995) [1] is shown in table 3.

The maximum fracture width in terms of the power law fluid parameters is given by:

$$w_f = 9.15^{\frac{1}{2n+2}} \times 3.98^{\frac{n}{2n+2}} \left(\frac{1+(\pi-1)n}{n} \right)^{\frac{n}{2n+2}} K^{\frac{1}{2n+2}} \times \left(\frac{(q_i/2)^{n_{h_f^{1-n_{x_f}}}}}{E'} \right)^{\frac{1}{2n+2}} \quad (2)$$

Where: E' is the plane strain in psi, $E' = \dfrac{1}{1-\nu^2}$;

n is the flow behavior index (dimensionless); K is the consistency index (Pa.sec^n); ν is in the Poisson's ratio; μ is in Pa.s. (Rahman, M. M., 2002), the power law parameters are correlated with fluid viscosity of fracturing fluid as [7]:

$$n = 0.1756 \times (\mu)^{-0.1233}$$

$$K = 47.880 \times (0.5\mu - 0.0159)$$

By using the shape factor of $\pi/5$ for a 2D PKN fracture geometry model, the average fracture width w_a is given by $\pi/5 \times w_f$ as equation.

$$w_a = \frac{\pi}{5} \times 9.15^{\frac{1}{2n+2}} \times 3.98^{\frac{n}{2n+2}} \left(\frac{1+(\pi-1)n}{n} \right)^{\frac{n}{2n+2}} K^{\frac{1}{2n+2}} \times \left(\frac{(q_i/2)^{n_{h_f^{1-n_{x_f}}}}}{E'} \right)^{\frac{1}{2n+2}} \quad (3)$$

Carter solution II formulated material balance in terms of injection rate to the well. At the injection time t_e, the injection rate enters one wing of the fracture area, the material balance presents the relationship between injection rate (q) of the total fracture volume with fluid volume losses to fractures. The material balance is presented as equation below.

$$q = 2 \int_0^t \frac{C_L}{\sqrt{t-\tau}} \times \left(\frac{dA}{d\tau} \right) d\tau + 2S_p \times \frac{dA}{dt} + w \times \frac{dA}{dt} + A \frac{dw}{dt} \quad (4)$$

By an analytical solution for constant injection rate (q), Cater solved the material balance that gives the fracture area for two wings as:

$$A(t) = \frac{w_a + 2S_p}{4C_L^2 \pi} \times q \left[exp(\beta^2) erfc(\beta) + \frac{2\beta}{\sqrt{\pi}} - 1 \right] \quad (5)$$

Hence fracture half-length with the fracture surface area $A(t) = 2x_f h_f$ is given by

$$x_f = \frac{w_a + 2S_p}{4C_L^2 \pi} \times \frac{q}{2} \left[exp(\beta^2) erfc(\beta) + \frac{2\beta}{\sqrt{\pi}} - 1 \right] \quad (6)$$

Where: $\beta = \dfrac{2C_L \sqrt{\pi t}}{w_a + 2S_p}$

Equation (6) presents the fracture half-length during proppant slurry injection into the fractures and this equation also describes the fracture propagation alongside the fractures with time. Accordingly, the fracture half-length depends on several parameters as injection rate (q), injection time (t), leak-off coefficient (C_L), spurt loss (S_p), fracture height (h_f), and the average fracture width (w_a). From the close of equation (6), it can be easy to determine the valuable fracture half-length by using iterative calculation method. The PKN fracture geometry model is presented in figure 1.

MATERIAL BALANCE

Cater solved the material balance to account for the leak-off coefficient, spurt loss, injection rate, injection time, and in terms of power law parameters of flow behavior index of n and consistency index of K. Proppant

slurry is pumped to the well under high pressure to produce fracture growth and fracture propagation. Therefore, the material balance is expressed as equation: $V_i = V_f + V_l$, where V_i is the total fluid volume injected to the well, V_f is the fracture volume that is required to stimulate reservoir, and V_l is the total fluid losses to the fracture area in the reservoir. The fracture volume, V_f, is defined as two sides of the symmetric fracture of

$V_f = 2x_f h_f w_a$ [1]. The fluid efficiency is defined by V_f/V_i. In 1986, Nolte proposed the relationship between the fluid volumes injected and pad volume as well as a model for proppant schedule. At the injection time t, the injection rate enters into two wings of the fractures with q, the material balance presented as the constant injection rates q is the sum of the different leak-off flow rate plus fracture volume [8] as:

$$q = 2\int_0^t \frac{C_L}{\sqrt{t-\tau}} \times \left(\frac{dA}{d\tau}\right) d\tau + 2S_p \times \frac{dA}{dt} + w \times \frac{dA}{dt} + A\frac{dw}{dt} \tag{7}$$

The fluid efficiency of fractured well of the post fracture at the time (t) is given by:

$$\eta = \frac{w_a h_f x_f}{qt} \quad \text{or} \quad \eta = \frac{w_a h_f \left(w_a + 2S_p\right)}{4\pi C_L^2 t} \times \left[exp\left(\beta^2\right) erfc\left(\beta\right) + \frac{2\beta}{\sqrt{\pi}} - 1\right] \tag{8}$$

Where: $\beta = \dfrac{2C_L\sqrt{\pi t}}{w_a + 2S_p}$, and C_L is the leak-off coefficient in ft/min$^{0.5}$, w_a is the average fracture width in the fractures in inch, S_p is the spurt loss in the fractures in gal/ft^2.

CENTRAL COMPOSITE DESIGN (CCD)

The design of experiments (DOE) techniques is commonly used for process analysis and the models are usually the full factorial, partial factorial, and central composite rotatable designs. An effective alternative to the factorial design is the central composite design (CCD), which was originally developed by Box and Wilson and improved by Box and Hunter in 1957. The CCD was widely used as a three-level factorial design, requires much fewer tests than the full factorial design, and has been provided to be sufficient as describing the majority of steady state products of response. Currently, CCD is one of the most popular classes of design used for fitting second-order models. The total number of tests required for is $2^k + 2k + n_0$, including the standard 2^k factorial points with its origin at the center, $2k$ points fixed axially at a distance, say β ($\beta = 2^{k/4}$), from the center to generate the quadratic terms, and replicate tests at the center (n_0), where k is the number of independent

variables. These operating parameters of the variables are named as injection rate, X_1, injection time, X_2, leak-off coefficient, X_3, presenting the total number of test required of the three variables of $2^3 + (2\times3) + 3 = 17$. In this experiment design, the center points were set at 3 and the replicates of zero value. Therefore, the three independent variables of the operating parameters of the CCD were shown in table 3. The coded and actual levels of the dependent variables of each experiment design in the matrix column are calculated in table 4. From table 4, the experiment of design is conducted for obtaining the response [9].

Table 4. Three independent variables and their levels for central composite design (CCD) [9]

	Coded variable level		
	Low	Center	High
Variables symbol	-1	0	1
Injection rate, bpm	18	19	20
Injection time, minutes	60	90	120
Leak-off coefficient, ft/min$^{0.5}$	0.003	0.005	0.007

THE EFFECTS OF OPERATING PARAMETERS OF HYDRAULIC FRACTURING ON THE FRACTURE GEOMETRY

Currently, the hydraulic fracturing in the field can be divided into two types of parameters as operating parameters of hydraulic fracturing of the injection rate, injection time and leak-off coefficient at which these parameters are controlled from the surface and facilities and the rest of parameters that cannot be controlled as rock properties of young modulus, geological structure, reservoir porosity, reservoir permeability and fracture closure pressure and the stress regime of the fracture of normal fault stress regime, strike slip regime, reverse faulting stress regime. In this article, the authors have presented the operating parameters on fracture geometry of fracture half-length at the normal faulting stress regime that is the minimum horizontal stress as closure pressure of 7,700 psi. In this research, the recommended operating parameters is based on the field experience offshore Vietnam for the injection rate in the range of 18 bpm to 22 bpm, injection time in the range of 60 minutes to 120 minutes, and the leak-off coefficient in the range of 0.003 ft/min$^{0.5}$ to 0.007 ft/min$^{0.5}$. One of the most important operating parameters is the leak-off coefficient at which the leak-off coefficient has more effect on the fracture geometry as well as on the net present value. Current total leak-off coefficient is controlled by three mechanisms of rock compressibility, invaded zone, and wall building effect. In the three mechanisms, only one parameter can control of filtration viscosity of fracturing fluid system. Usually, the higher fracturing fluid viscosity as high polymer concentration of the fracturing fluid that is the same as high fracturing fluid density can decrease the wall building effect as the decrease in the total leak-off coefficient. In this research, the author proposed the fracturing fluid parameters and fluid properties as in the table 2.

The model for overall leak-off coefficient was presented by (Williams, 1970 and Williams et al., 1979) [10-12] as:

$$C_l = \frac{-\dfrac{1}{C_c} + \sqrt{\dfrac{1}{C_c^2} + 4\left(\dfrac{1}{C_v^2} + \dfrac{1}{C_w^2}\right)}}{2\left(\dfrac{1}{C_v^2} + \dfrac{1}{C_w^2}\right)} \qquad (9)$$

Where: C_v is the viscous fluid loss coefficient due to the filtration in ft/min$^{0.5}$; C_w is the wall building of fluid loss coefficient in ft/min$^{0.5}$; C_c is leak-off coefficient due to total compressibility in ft/min$^{0.5}$.

THE EFFECTS OF THE INJECTION RATE ON THE FRACTURE GEOMETRY

Figure 2 and figure 3 present the effect of the injection rate on the fracture half-length, fracture width. These figures demonstrates that when the increase in the injection rate changes from 18 bpm to 22 bpm to the well, there is the increase in the fracture half-length. Meanwhile, the injection rate decreases from 22 bpm to 18 bpm there is also the decrease in the fracture half-length. This is because that the injection rate is directly proportional to the fracture half-length. This explains why the injection rate increases from 18 bpm to 22 bpm, the fracture half-length increases. In which the fracture height is constant of 72 ft during injection to the well and injection time is originated by the design of injection time with the fracture geometry of 2D PKN-C. Figure 2 has demonstrated when there is the increase in the injection rate, fracture half-length also increases. This is because that the fracture half-length is directly proportional to the fracture width. In the figure 4 presents the injection rate versus the fluid efficiency in terms of the 2D PKN-C fracture geometry model. The figure has illustrated that when the injection rate increases from 18 bpm to 20 bpm, the fluid efficiency increases because the fracture volume is gradually higher than the total volume injected to the well as low fluid loss volume in the fractures. This leads to the increase in the fluid efficiency. Accordingly, the injection rate ranges from 20 bpm to 22 bpm, the fluid efficiency decreases due to high injection rate to the well as high pressure injected into the wells. This leads to high total fluid loss volume into the fractures as narrow fracture volume of the material balance.

The relationship between the response of the fracture half-length, fracture width and fluid efficiency with these variables has been presented in equation 1 and equation 2, respectively.
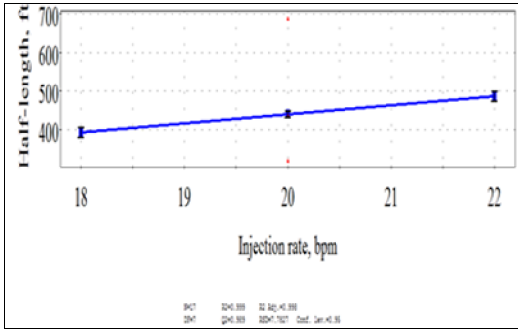
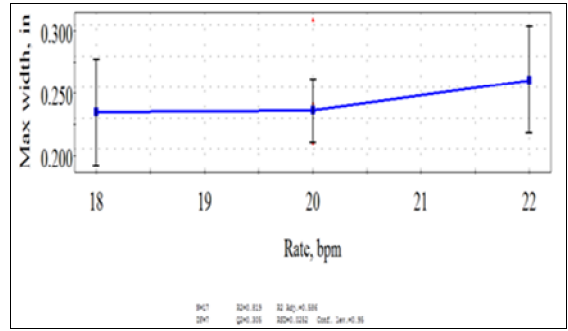**Fig. 2.** The effect of injection rate on the fracture half-length

Fig. 3. The effect of injection rate on fracture width

Table 5. Independent variables and results of post fracture production with simulation observed by Central Composite Design (CCD) [13, 14]

Run	Coded level of the variables			Actual level of variables			Response (simulation and observed)		
	X_1	X_2	X_3	Injection rate, bpm	Injection time, minutes	Leak-off coefficient, ft/min$^{0.5}$	Fracture-half length, ft	Fracture width, in	Fluid efficiency, %
1	-1	-1	-1	18	60	0.003	499.9	0.274	15
2	1	-1	-1	22	60	0.003	602.7	0.301	16.3
3	-1	1	-1	18	120	0.003	727.2	0.308	12.3
4	1	1	-1	22	120	0.003	879.0	0.340	13.4
5	-1	-1	1	18	60	0.007	235.3	0.212	5.55
6	1	-1	1	22	60	0.007	286.1	0.237	6.1
7	-1	1	1	18	120	0.007	336.1	0.241	4.43
8	1	1	1	22	120	0.007	409.2	0.209	4.86
9	-1	0	0	18	90	0.005	396.6	0.200	7.35
10	1	0	0	22	90	0.005	481.6	0.280	8.04
11	0	-1	0	20	60	0.005	355.0	0.250	8.75
12	0	1	0	20	120	0.005	510.4	0.280	13.92
13	0	0	-1	20	90	0.003	687.8	0.309	14
14	0	0	1	20	90	0.007	321.5	0.242	5.1
15	0	0	0	20	90	0.005	439.2	0.21	7.71
16	0	0	0	20	90	0.005	439.2	0.21	7.71
17	0	0	0	20	90	0.005	439.2	0.21	7.71

$$Fracture\ half-length = 46.35X_1 + 88.29X_2 - 180.84X_3 - 0.54X_1^2$$
$$- 6.94X_2^2 + 65.011X_3^2 + 8.91X_1X_2 - 16.33X_1X_3 - 34.96X_2X_3 \tag{10}$$

$$Fracture\ width = 0.231465 + 0.0132X_1 + 0.0104X_2 - 0.0391X_3 - 0.00756X_1^2$$
$$+ 0.01744X_2^2 + 0.02794X_3^2 - 0.0065X_1X_2 - 0.00825X_1X_3 - 0.009X_2X_3 \tag{11}$$

$$Fluid\ Efficiency = 8.48 + 0.407X_1 - 0.279X_2 - 4.496X_3 - 1.36275X_1^2 + 2.27725X_2^2$$
$$+ 0.492253X_3^2 - 0.04X_1X_2 - 0.1775X_1X_3 + 0.405X_2X_3 \tag{12}$$

The equations 10, 11, and 12 have shown the relationship between the responses of the fracture half-length, fracture width, and fluid efficiency respectively with the variables that

are presented in the detail of the figures 2, 3, and 4. Moreover, the figure 5 can be divided into two regions. The first region presents the negative factor of these variables of X_1, $X_2.X_3$, $X_1.X_3$, $X_2.X_2$, and $X_1.X_1$. The increase of the factors results in the decrease in the fracture half-length. Accordingly, the decrease of the factors of the variables leads to the increase in the fracture half-length. The second region describes the positive factors of these variables of X_2, $X_3.X_3$, X_1, $X_1.X_2$ that effect the increase of fracture half-length. The increase of the positive factors of the fracture width model (11) leads to the increase of fracture width and increase of the fracture half-length because fracture width is directly proportional to the fracture half-length. The negative factors of these variables of X_3, $X_2.X_3$, $X_1.X_3$, $X_1.X_1$, $X_1.X_2$ effect the decrease of the fracture width. Figure 5 presents these factors of the variables affecting the fluid efficiency that shows the relationship between the variables and the fluid efficiency as presented in equation (12). The figure is also divided into two regions. The first region presents of the positive factors of $X_2.X_2$, $X_3.X_3$, X_1, $X_2.X_3$ that affect the increase of the fluid efficiency. Whereas, the second region presents the negative factors of these variables of X_2, X_3, $X_1.X_1$, $X_1.X_2$, $X_1.X_3$, that affect the decrease of the fluid efficiency. Especially, higher leak-off coefficient leads to low fluid efficiency. This is because the higher leak-off coefficient and higher total fluid volume loss in the fractures during proppant slurry injected to the well under high pressure lead to low fracture volume as understanding in the material balance.
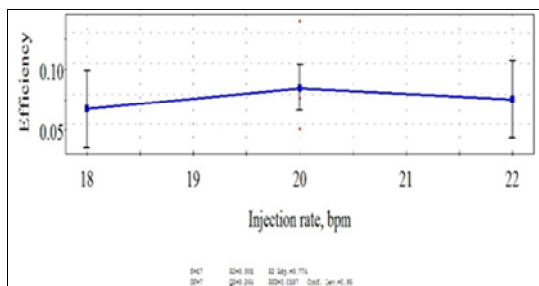

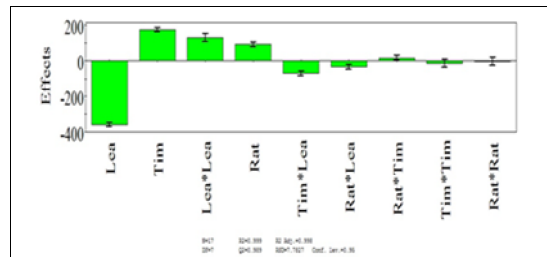**Fig. 4.** The effect of injection rate on fluid efficiency

Fig. 5. The plots of the effect of these variables on the fracture half-length
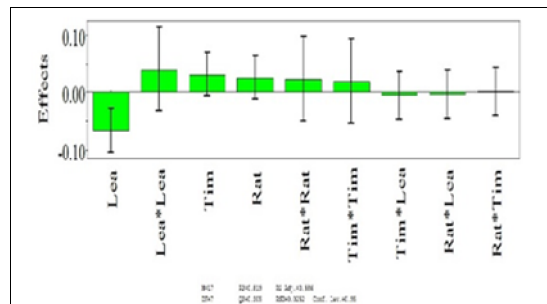

Fig. 6. The plots of the effect of these variables on the fracture width
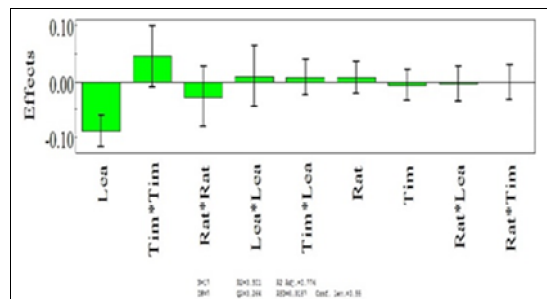

Fig. 7. The plots of the effect of these variables on fluid efficiency

THE EFFECT OF THE INJECTION TIME ON THE FRACTURE GEOMETRY

The effects of injection time on fracture half-length and fracture width are presented in figures 8, and 9, respectively. This explanation is when injection time increases from 60 minutes to 120 minutes, the fracture half-length increases. Accordingly, the injection time increases, the fracture width increases gradually. This is because the injection time is directly proportional to fracture half-length. The more injection time results in long fracture

half-length. Because the fracture width is directly proportional to the fracture half-length the more inection time leads to wider fracture width and longer fracture half-length. The long injection time leads to increase in the fracture volume besides the volume loss into the fractures. The relationship between the variables of X_1, X_2, X_3 and the response of the fracture geometry, fluid efficiency can be presented in equations (10) and (12).
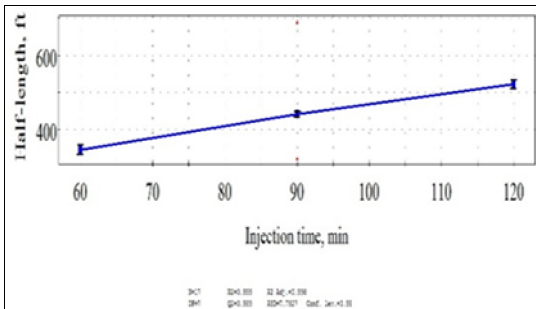

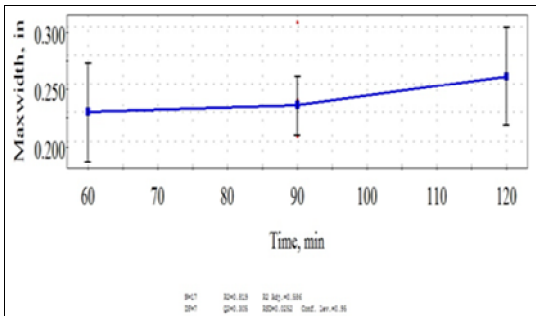**Fig. 8.** The effect of the injection time on the fracture half-length

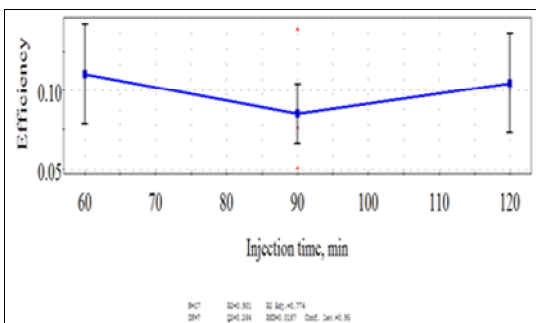**Fig. 9.** The effect of the injection time on the fracture width

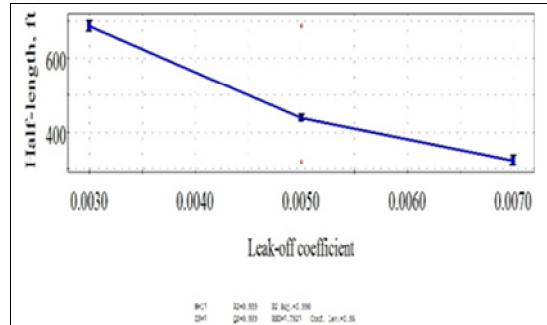**Fig. 10.** The effect of the injection time on fluid efficiency

Fig. 11. The effect of the leak-off coefficient on fracture half-length

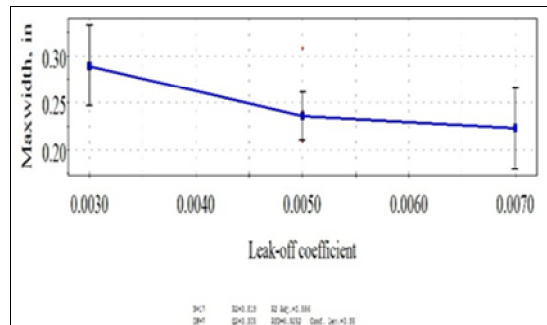## THE EFFECT OF LEAK-OFF COEFFICIENT ON THE FRACTURE GEOMETRY

Fig. 12. The effect of the leak-off coefficient on fracture width
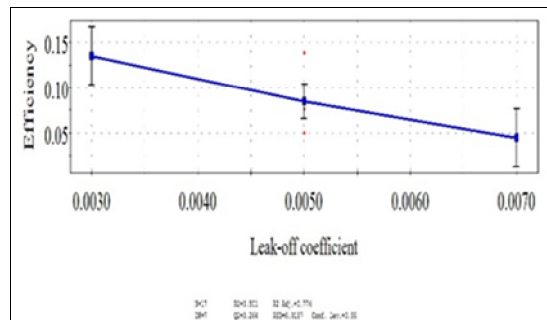

Fig. 13. The effect of the leak-off coefficient on the fluid efficiency

Figures 12 and 13 are present the effect of the leak-off coefficient on the fracture geometry. The figures explain when the leak-off coefficient C_1 increases from 0.003 ft/min$^{0.5}$ to 0.007 ft/min$^{0.5}$, the fracture

half-length decreases. Accordingly, the decrease of fracture half-length results in decrease of fracture width because fracture half-length is directly proportional to the fracture width as presented in figure 8. This is because the increase of the leak-off coefficient leads to decrease of fracture half-length because leak-off coefficient is inversely proportional to fracture half-length as presented in figure 3. In another explanation, based on the material balance, the total injection rate q is equal to fracture volume and fluid volume loss among the fractures. Thus, the larger leak-off coefficient caues larger fluid volume loss. higher leak-off coefficient leads to more fluid volume loss to the fractures because the leak-off coefficient is proportional to the total fluid volume loss and thin fracture geometry as shorter fracture half-length. This is based on the 2D PKN fracture geometry in terms of the leak-off coefficient and power law parameters. Meanwhile proppant slurry is pumped into the well under high pressure based on the constant fracture height of 72 ft. Figure 13 presents the leak-off coefficient versus the fluid efficiency. The figure has shown when the leak-off coefficient increases from 0.003 ft/min$^{0.5}$ to 0.007 ft/min$^{0.5}$, the fluid efficiency decreases. This is because the larger leak-off coefficient results in more fluid volume loss into the area of the fractures. Meanwhile, the material balance is equal to the fracture volume plus the total fluid volume loss. Thus more total fluid volume loss brings to low fluid efficiency. Furthermore, the fluid efficiency is given by [15].

$$Fluid\ efficiency = \frac{V_f}{V_i} = \frac{Vi - V_l}{V_i} = 1 - \frac{V_l}{V_i} \qquad (13)$$

CONCLUSIONS

Through this research of design of experiments (DOE), that applies the operating parameters of hydraulic fracturing to evaluate the effect of parameters on the fracture geometry and fluid efficiency of using the 2D PKN-C fracture geometry model, the authors can summarize as follows.

The increase of the injection rate leads to increase of the fracture half-length and fracture width, and the gradual decrease of the fluid efficiency.

The increase of the injection time brings to increase of the fracture half-length, fracture width, and decrease of the fluid efficiency.

The higher leak-off coefficient results in narrower fracture width, shorter fracture half-length, and low fluid efficiency.

REFERENCES

1. *Valk, P., and Economides, M. J., 1995.* Hydraulic fracture mechanics. Wiley, New York.

2. *Nguyen, D. H., and Bae, W., 2013.* Design Optimization of Hydraulic Fracturing for Oligocene Reservoir in Offshore Vietnam. In IPTC 2013: International Petroleum Technology Conference.

3. *Economides, M., Oligney, R., and Valkó, P., 2002.* Unified fracture design: bridging the gap between theory and practice. Orsa Press.

4. *Perkins, T. K., and Kern, L. R., 1961.* Widths of hydraulic fractures. Journal of Petroleum Technology, **13**(9): 937-949.

5. *Nordgren, R. P., 1972.* Propagation of a vertical hydraulic fracture. Society of Petroleum Engineers Journal, **12**(4): 306-314.

6. *Howard, G. C., and Fast, C. R., 1957.* Optimum fluid characteristics for fracture extension. In Drilling and production practice. American Petroleum Institute.

7. *Rahman, M. M., and Rahman, M. K., 2010.* A review of hydraulic fracture models and development of an improved pseudo-3D model for stimulating tight oil/gas sand. Energy Sources, Part A: Recovery, Utilization, and Environmental Effects, **32**(15): 1416-1436.

8. *Nolte, K. G., 1986.* Determination of proppant and fluid schedules from fracturing-pressure decline. SPE Production Engineering, **1**(4): 255-265.

9. *Myers, R. H., Montgomery, D. C., and Anderson-Cook, C. M., 2016.* Response surface methodology: process and product

optimization using designed experiments. John Wiley & Sons.

10. *Williams, B. B., 1970*. Fluid loss from hydraulically induced fractures. Journal of Petroleum Technology, **22**(07): 882-888.

11. *Williams, B. B., Gidley, J. L., and Schechter, R. S., 1979*. Acidizing fundamentals. Henry L. Doherty Memorial Fund of AIME, Society of Petroleum Engineers of AIME.

12. *Truong, N. H., Bae, W., and Nhan, H. T., 2016*. Integrated Model Development for Tight Oil Sands Reservoir with 2D Fracture Geometry and Reviewed Sensitivity Analysis of Hydraulic Fracturing. Research Journal of Applied Sciences, Engineering and Technology, **12**(4): 375-385.

13. *Meyer, 2014*. Fracturing Simulation. Mfrac Software.

14. *Smith, M. B., 1997*. Hydraulic Fracturing. 2nd Edn., NSI Technologies, Tulsa, Oklahoma

15. *Economides, M. J., and Martin, T., 2007*. Modern fracturing: Enhancing natural gas production (pp. 978-1). Houston, Texas: ET Publishing.

ẢNH HƯỞNG CỦA CÁC THÔNG SỐ VẬN HÀNH NỨT VỈA THỦY LỰC LÊN HÌNH DÁNG NỨT VỈA VÀ HIỆU QUẢ NỨT VỈA CHO TẦNG CHỨA OLIGOCEN TẠI VÙNG BIỂN VIỆT NAM

Nguyễn Hữu Trường

Trường Đại học Dầu khí Việt Nam

   TÓM TẮT: *Trong những thập kỷ qua, một lượng lớn dầu được khai thác tại bồn trũng Cửu Long chủ yếu từ tầng móng, và một lượng nhỏ dầu được khai thác tại tầng chứa Miocen và tầng chứa dầu Oligocen. Nhiều giếng thăm dò và giếng khai thác thuộc Trà Tân và Trà Cú thuộc đối tượng Oligocen cát kết có tiềm năng chứa dầu khí tốt, tại đó đa số các vỉa chứa dầu có độ rỗng trung bình khoảng từ 10% đến 18%, và độ thấm của vỉa chứa khoảng 0,1 md đến 5 md. Do cấu trúc địa chất của các vỉa dầu khí bất đồng nhất và phức tạp ở đó áp suất đóng khe nứt lên đến 7.700 psi nhưng cho lưu lượng khai thác dầu còn hạn chế. Vấn đề lớn của vỉa chứa dầu thuộc đối tượng Oligocen là dẫn suất của các khe nứt trong vỉa chứa rất thấp do độ liên thông của các khe nứt trong vỉa chứa dầu khí kém. Để giải quyết những thách thức lớn này cần phải kích thích vỉa dầu khí bằng nứt vỉa thủy lực để khơi thông các khe nứt nhằm nâng cao lưu lượng khai thác. Trong bài viết này, tác giả trình bày ảnh hưởng của các thông số vận hành nứt vỉa thủy lực như thời gian bơm nứt vỉa thủy lực, lưu lượng bơm, hệ số tốc độ mất dung dịch trên cơ sở mô hình 2D PKN-C, giới hạn bởi hệ số tốc độ mất dung dịch qua diện tích khe nứt, hệ số mất nước Sp, và các thông số mô hình power law lên hình dáng của khe nứt, với thiết kế thí nghiệm cho ba thông số vận hành nứt vỉa thủy lực dựa trên kinh nghiệm nứt vỉa thủy lực cho các vỉa dầu và áp dụng công cụ phương pháp bề mặt. Những năm gần đây, việc áp dụng thành công công nghệ nứt vỉa thủy lực để nhằm kích thích vỉa cho các giếng khoan hoàn thiện thuộc đối tượng Oligocen để nâng cao lưu lượng khai thác.*

   Từ khóa: *Thông số vận hành nứt vỉa thủy lực, hình dáng nứt vỉa 2D PKN-C, hiệu quả nứt vỉa.*